Transparent Quasi-Interdigitated Electrodes for Semi-transparent Perovskite Back-Contact Solar Cells

Giovanni DeLuca, a,b,c‡ Askhat N. Jumabekov, b‡ Yinghong Hu,b,d Alexandr N. Simonov, e,f Jianfeng Lu,c Boer Tan,c Gede W. P. Adhyaksa,g Erik C. Garnett,g Elsa Reichmanis, a,h* Anthony S. R. Chesman. b,i* and Udo Bach C,i,j*

^a School of Chemistry and Biochemistry, Georgia Institute of Technology, Atlanta, Georgia, United States

^b CSIRO Manufacturing, Clayton, Victoria, Australia.

^c Department of Chemical Engineering, Monash University, Clayton, Victoria, Australia.

^d Department of Chemistry and Center for NanoScience (CeNS), LMU Munich, Munich, Germany

^e School of Chemistry, Monash University, Clayton, Victoria, Australia

^f ARC Centre of Excellence for Electromaterials Science, Monash University, Clayton, Victoria, Australia

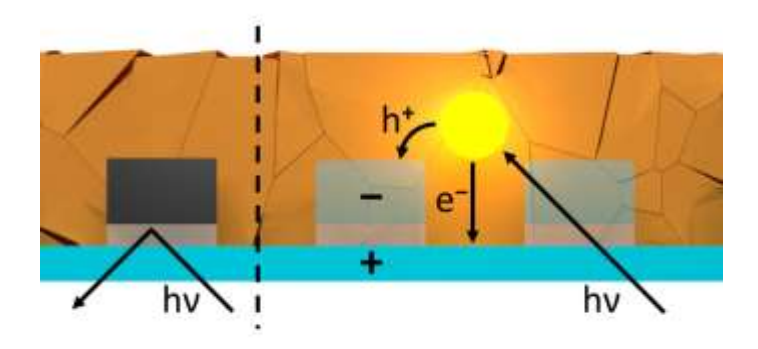
^g Center for Nanophotonics, AMOLF, Amsterdam, The Netherlands

^h School of Chemical and Biomolecular Engineering, Georgia Institute of Technology, Atlanta, Georgia, United States

ⁱ Melbourne Centre for Nanofabrication, Clayton, Victoria, Australia

^j ARC Centre of Excellence for Exciton Science, Monash University, Victoria, Australia

^{*} Corresponding authors. E-mail address: udo.bach@monash.edu (U. Bach), elsa.reichmanis@chbe.gatech.edu (E. Reichmanis), anthony.chesman@csiro.au (A. S. R. Chesman).



Transparent quasi-interdigitated electrodes (t-QIDEs) were produced by replacing the opaque components of existing QIDEs with indium tin oxide (ITO). We demonstrate their application in the first semi-transparent back-contact perovskite solar cell. A device with a $V_{\rm OC}$ of 0.88 V and a $J_{\rm SC}$ of 5.6 mA cm⁻² produced a modest 1.7 % efficiency. The use of ITO allows us to illuminate the device from front- and rear-sides, resembling a bifacial solar cell, both of which yield comparable efficiencies. Coupled optoelectronic simulations reveal this architecture may achieve power conversion efficiencies of up to 11.5 %, and 13.3 % when illuminated from front- and rear-side, respectively, using a realistic quality of perovskite material.

[Keywords]: Back contact solar cell, perovskite solar cell, coupled optical—electrical modeling, transparent conducting oxides, transparent quasi-interdigitated electrodes

[‡] Contributed equally to this work.

While back-contact electrodes (BCEs) are incorporated into the highest efficiency silicon solar cells,¹ they are yet to be adopted by researchers fabricating organometal halide perovskite analogues. This is despite simulations predicting back-contact perovskite solar cells (BC-PSCs) may have higher theoretical efficiencies than conventional sandwich structures due to the removal of parasitic light absorption from top contacts.² Furthermore, the architecture offers several functional advantages during fabrication, including the elimination of shorting due to pinholes, and avoiding damage to the perovskite layer during the deposition of subsequent layers.³ However, the electrode spacing in the BCEs currently used in Si solar cells is too large for perovskites which have shorter carrier diffusion lengths. Also, the processes used to fabricate commercial BCEs are not compatible with perovskite thin films,⁴ thus prohibiting the direct transfer of existing technology to this new class of photoabsorber material.

The realization of an operational BC-PSC therefore necessitated the development of a new device architecture, namely quasi-interdigitated electrodes (QIDEs) (Figure 1a). This back-contact architecture places a finger-shaped cathode onto a continuous thin-film anode, with an insulating layer separating the two electrodes. This structure avoids formation of the short-circuit pathways that occur in conventional co-planar interdigitated electrodes when a defect in one electrode finger causes contact with an adjacent electrode, a problem that increases in frequency as the electrode features are miniaturized to the dimensions required for the charge carrier diffusion lengths of perovskites.³

Although the QIDEs present a robust architecture for BC-PSCs, a key element of the design places limits on potential applications. The top contacts of currently available QIDEs are comprised of opaque Al/NiCo fingers, which are strong absorbers/reflectors of incident light (Figure 1b), preventing their use in semitransparent PSCs or as the top electrode in tandem

perovskite-silicon solar cells. As a result, for QIDEs to reach their full potential, this top electrode must be replaced with a transparent conducting material. To this end, we introduced herein the first transparent quasi-interdigitated electrode (t-QIDEs) based on indium tin oxide (ITO), which has a high carrier concentration, low sheet resistance, and, most importantly, higher optical transmittance (>85% in visible wavelengths) than Al/NiCo.⁵ Furthermore, we demonstrated the first operational semi-transparent back-contact perovskite solar cell based on t-QIDEs. Optoelectronic theoretical simulations⁶ showing the realistically achievable power conversion efficiencies (PCEs) and average visible transmission (%AVT) at varying perovskite film thicknesses are also provided.

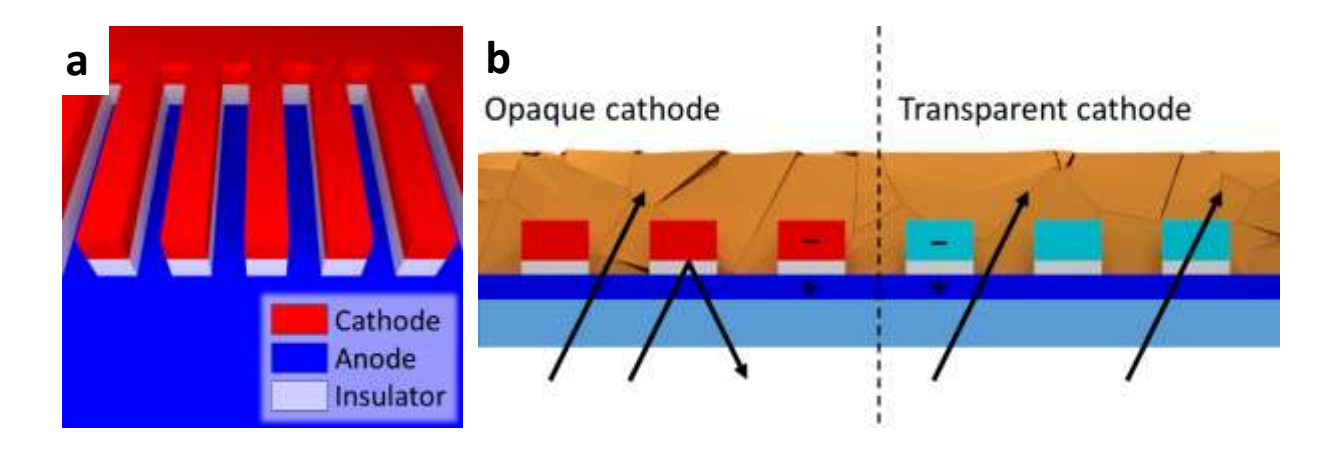


Figure 1. (a) The structure of a QIDEs. (b) Light transmission, absorption and reflection in QIDEs with Al/NiCo electrodes (left) or transparent electrodes (right).

Creating a t-QIDE first required optimization of the radio frequency magnetron sputtering deposition of ITO that was to replace the opaque components in the original architecture. Optimization was achieved by varying the following deposition parameters: substrate

temperature, ITO target power, argon and oxygen flow rates, and post-deposition annealing conditions. The optimized process yielded ~200 nm ITO thin films with an optical transmittance of ca. 88% at 592 nm (Figure S1), and sheet resistances ranging from 25 to 35 Ω square⁻¹. Photoelectron spectroscopy in air (PESA) measurements confirmed the ITO had a work function (4.78 ± 0.08 eV) comparable to literature values (Figure S2 and Table S1).⁷

Post-deposition annealing for 3 minutes in at 300 °C was required to enhance transmittance in the solar spectrum region (Figure S1). This change in transmittance is accompanied by the transformation of fully amorphous ITO to a highly crystalline phase, as evidenced by X-ray diffraction (XRD) measurements (Figure S3). In addition, post-deposition annealing resulted in a twentyfold decrease in sheet resistance. While heating the substrate during ITO deposition is preferable to a post-deposition annealing treatment^{8,9} to afford larger grains and minimize grain boundaries that may hinder electron mobility, the high temperatures required for the former process are not compatible with the photoresist used during t-QIDEs fabrication, therefore the sample required the post-annealing process.

Once optimized, the deposition parameters were applied to the fabrication of the ITO fingers for t-QIDEs. The initial electrode fabrication steps followed previously reported work,³ where a photoresist served as the negative of the electrode pattern applied to a TiO₂/FTO stack on a glass substrate, followed by the deposition of an Al₂O₃ insulating layer to separate the anode and cathode. A continuous thin film of ITO was then deposited, and subsequent lift-off of the photoresist mask afforded ITO electrode fingers. Visible light microscope images taken following lift-off revealed that the mask was completely removed, and the ITO fingers were undamaged (Figure S4). After removing the photoresist mask, the electrodes were annealed, transforming the electrodes from light-brown to colorless (Figure 2a). Finally, to ensure the

electrodes have the necessary band energy alignment with a perovskite photoabsorber, a suitable hole transport material, copper (I) thiocyanate, was electrodeposited onto the ITO fingers prior to perovskite deposition.

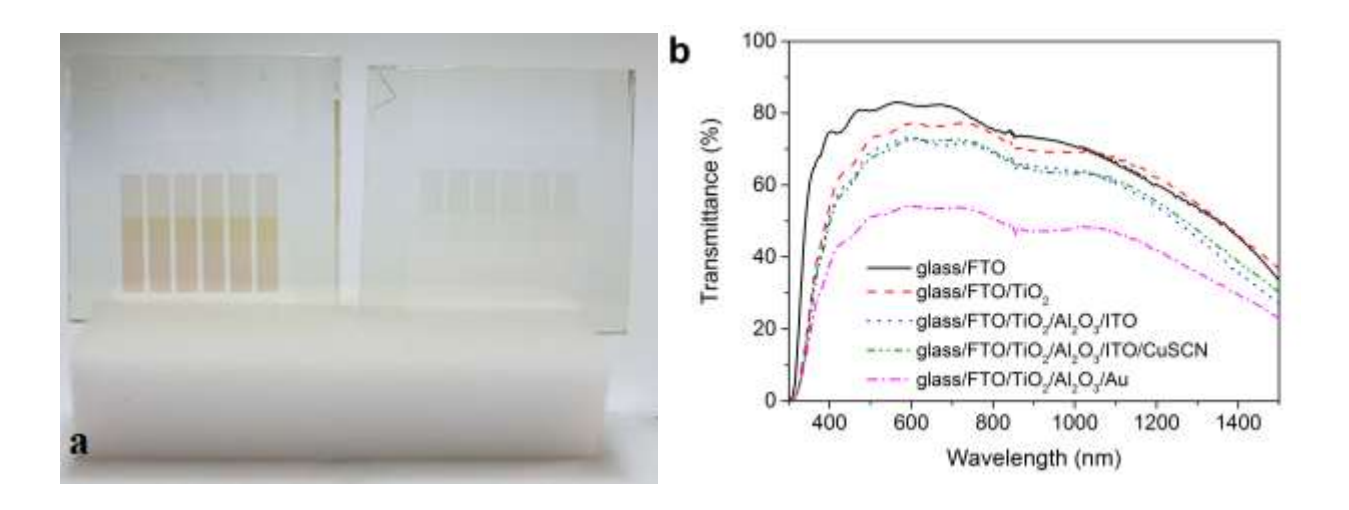


Figure 2. (a) Photograph of t-QIDEs before (left) and after annealing at 300 °C (right). (b) UV-Vis-NIR transmission spectra of the t-QIDEs at various stages of fabrication (black, red, blue, green), and for a QIDEs with a gold top electrode instead of ITO (magenta).

UV-Vis-NIR spectroscopy measurements were performed on the electrode stack at each stage of the fabrication process to determine the contribution of each component to the incident light absorption of the t-QIDEs (Figure 2b, Table S2 and Table S3). The pristine FTO-coated glass exhibited the highest transmittance, while TiO₂ deposition resulted in a slight drop in transmittance in the blue and visible regions of the spectrum. After depositing the Al₂O₃/ITO top electrode (quasi-interdigitated area), the overall transmittance decreased by approximately 15% and 10%, relative to the FTO glass substrate and FTO/TiO₂ anode, respectively. This results from the formation of additional interfaces (TiO₂/Al₂O₃ and Al₂O₃/ITO), which enhance the

reflectance of the electrode assembly. The addition of the hole transport layer caused insignificant changes to the transmittance (Figure 2b), and the average transmittance in the range 530–1100 nm, which is most important from the perspective of photovoltaic application, remained at *ca.* 68%. The employed t-QIDE architecture is an ordinary reciprocal system and the transmission through both sides should give identical results, which was indeed the case, with insignificant differences most probably arising from scattering (Figure S5). To demonstrate the transparency of the ITO fingers, identical measurements were performed on a device where ITO was replaced with a *ca.* 60 nm thick layer of gold. This substitution resulted in a significant decrease in transmission to *ca.* 50%, confirming that the relatively high transmittance of the t-QIDEs is due to the transparent nature of ITO (Figure 2b).

While t-QIDEs could potentially be applied to a range of photoabsorber materials, CuSCN was applied to the ITO to provide for a band energy alignment compatible with a hybrid organic-inorganic perovskite (Figures S6 and S7). For this study we selected a multiple-cation mixed-halide perovskite with the nominal composition Cs_{0.05}FA_{0.79}MA_{0.16}PbI_{2.49}Br_{0.51} as the photoabsorber, which has been shown to result in high photovoltaic efficiencies.¹⁰ Figure 3a presents a cross-sectional scanning electron micrograph of a back-contact PSC based on t-QIDEs. The back-scattered electron image of an individual finger reveals that a thin perovskite photoabsorber layer (~340 nm) uniformly covers the surface of the t-QIDE, which consists of a microstructured cathode (~1.5 μm wide ITO/CuSCN micro-fingers spaced every ~2.5 μm) on a continuous anode (FTO/TiO₂ on a glass substrate), separated by ~100 nm thin layer of Al₂O₃ (Figure S8). The micro-fingers of the cathode were found to be trough shaped rather than perfectly flat. This is the consequence of the employed polymer mask fabrication process where the edges of the grooves formed by the mask are imperfectly defined. While this is anticipated to

impede the device performance to some extent, it can be alleviated through optimization of the polymer mask fabrication process. A back-scattered electron cross-section image provides additional contrast to differentiate the functional device layers (Figure 3c).

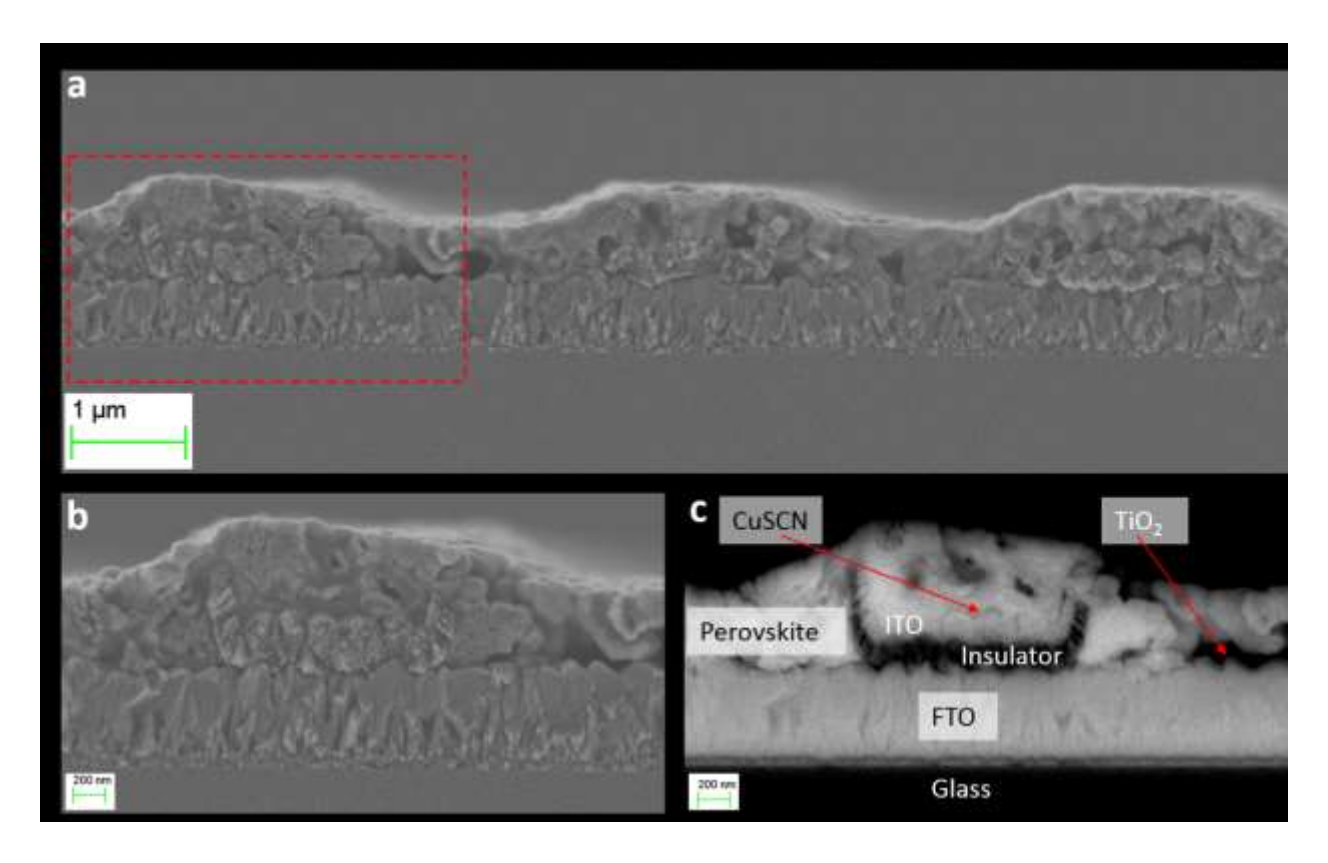
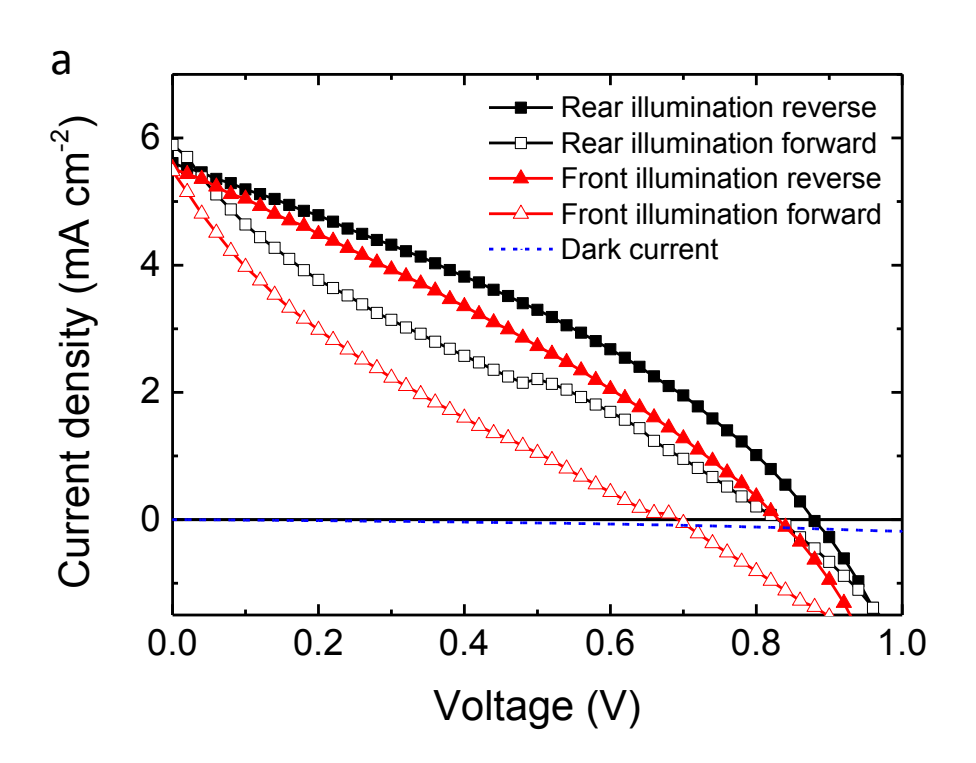


Figure 3. (a) Cross-sectional SEM image of the back-contact PSC based on the Cs_{0.05}FA_{0.79}MA_{0.16}PbI_{2.49}Br_{0.51} light-absorber and t-QIDE, (b) high magnification cross-sectional SEM image of the device (area enclosed with red rectangle in Figure 3a), (c) Back-scattered SEM cross-sectional image of an individual finger of the device (area enclosed with red rectangle in Figure 3a).

The *J-V* characteristics of back-contact PSCs with t-QIDEs were recorded with both front (perovskite) and rear (glass) side illumination. Figure 4a shows *J-V* curves under 1 sun AM1.5G illumination and in the dark, while relevant photovoltaic parameters are summarized in Table S4. With front side illumination, values of 5.5 mA cm⁻², 0.84 V and 30% were recorded for short-circuit current density (J_{SC}), open-circuit voltage (V_{OC}) and fill factor (FF), respectively, yielding

a PCE value of 1.4% for a reverse scan. For rear side illumination and reverse scan, a slightly higher PCE value of 1.7% was obtained, with J_{SC} , V_{OC} and fill factor being 5.6 mA cm⁻², 0.88 V and 34%, respectively. As expected, excluding CuSCN from t-QIDEs resulted in lower device performance, demonstrating the advantages provided by having a hole-selective layer (Figure S9). The J-V curves exhibit a hysteresis, which is typically assigned to ion migration and interfacial charge recombination. The maximum power point (MPP) for the best-performing device irradiated with 1 sun from rear showed a stable output with a PCE value of ca 1.2% maintained for at least 140 s (Figure 4b).



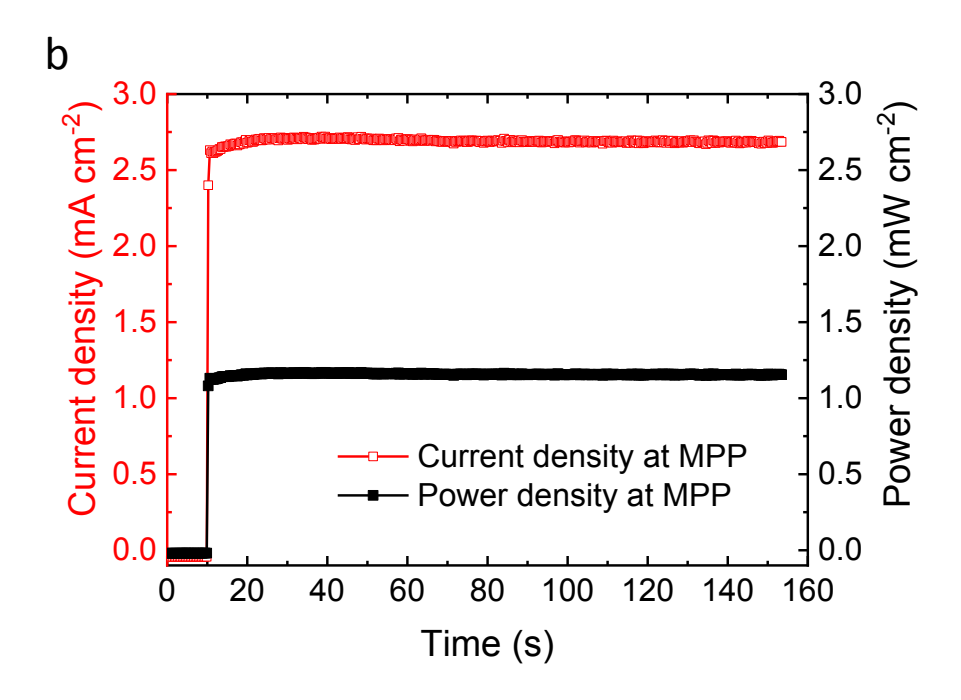


Figure 4. (a) J–V characteristics (scan rate 0.2 V s⁻¹) of a back-contact PSC based on the $Cs_{0.05}FA_{0.79}MA_{0.16}PbI_{2.49}Br_{0.51}$ light-absorber and a t-QIDE measured under 1 sun illumination from the front (perovskite) side and rear (glass) side, and in the dark. (b) Evolution of photocurrent and power density of the same BC-PSC at maximum power point under 1 sun irradiation from the rear side.

A potential application of t-QIDEs is in semi-transparent perovskite solar cells. While the PCEs of the current devices are notably below the state-of-the-art for back-contact solar cells, future increases in efficiency are anticipated through increased perovskite grain size, decreased sheet resistance of the transparent electrodes, and improved deposition procedures for the hole transport layer. To determine whether our device architecture could realistically reach the PCE and average visible transmission (%AVT) of the previously reported semi-transparent solar cells, ^{13,14} coupled optical and electrical simulations were performed following the published approach and previously reported physical characteristics for key components (Table S5). ⁶

The simulations used a realistic quality of perovskite material with a minority carrier diffusion length of 500 nm. Figure 5a shows the simulated evolution of PCE as a function of

perovskite layer thickness with a t-QIDE with the characteristics as used in this study. The simulations revealed an overall efficiency that is always higher when the cell is illuminated from the glass/electrode interface (rear-illumination) vs. the air/perovskite interface (front-illumination), which supports the experimental observations. A fluctuation in the PCE originates from a combination of thin-film interferences and drift-diffusion carrier transport, and becomes more pronounced with rear-illumination due to a higher number of modes evolved passing through the multilayer structure. When the device is illuminated from the front or rear side, the simulated maximum efficiency is *ca.* 12% (at 750 nm perovskite thickness) or *ca.* 13% (at 650 nm perovskite thickness), respectively. Rear-illumination requires a ~50 nm thinner perovskite layer to reach a similar efficiency to front-illumination, which also suggests more efficient charge collection.

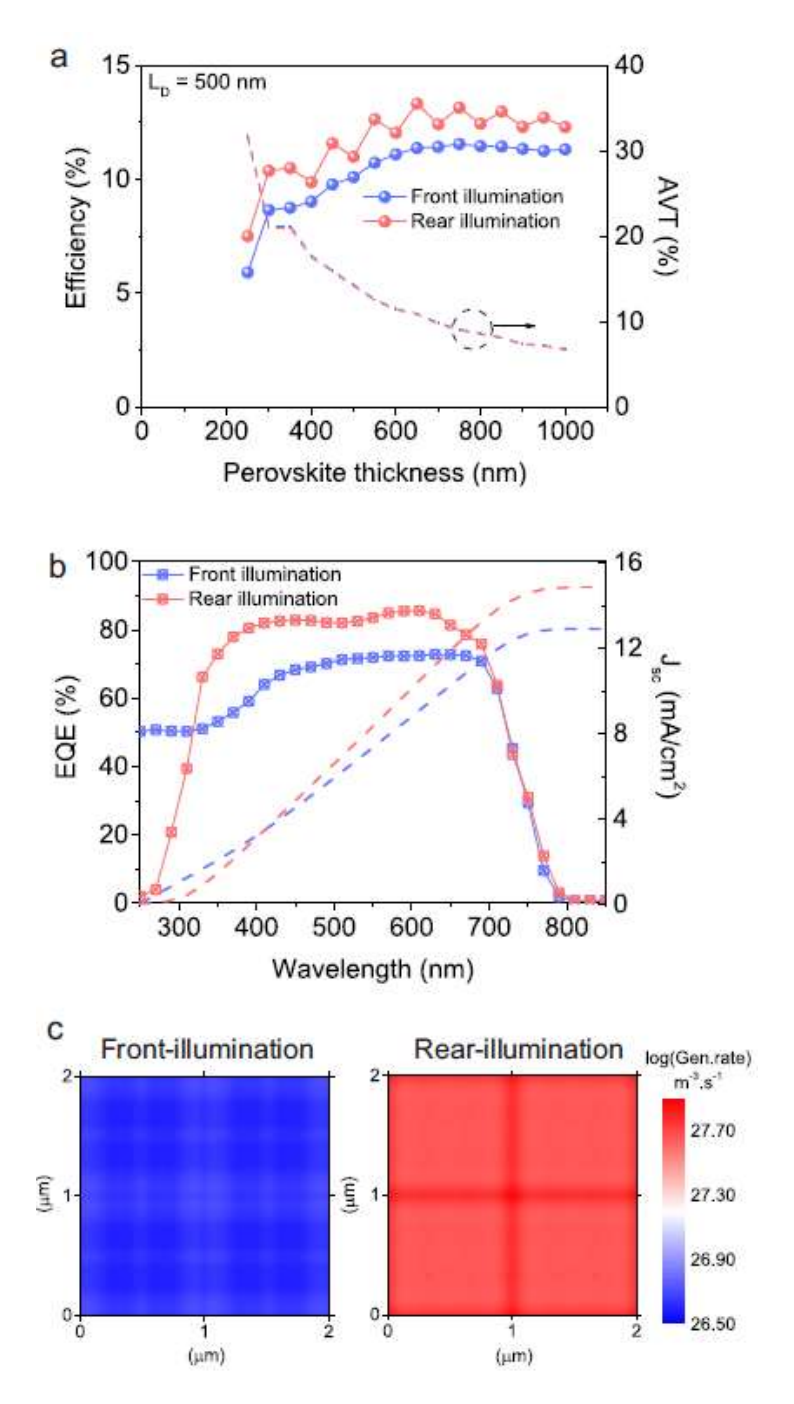


Figure 5. Simulated performance of a back-contact perovskite solar cell under front and rear illumination. (a) Power conversion efficiency and average visible transmittance as a function of perovskite thickness (the perovskite thickness cannot be below the thickness of the back-contact electrode, *viz.* 250 nm). Simulations were based on AM 1.5 spectrum and 500 nm minority—carrier diffusion length for the perovskite. (b) External quantum efficiency (EQE) at the optimum thickness of the perovskite layer (750 and 650 nm for the front- and rear-illumination, respectively). (c) Charge generation rate of the perovskite layer in between the two back-contact electrodes. The generation rate is averaged over the thickness of the perovskite and leveled to the total thickness of the electrodes.

Figure 5a also demonstrates the potential of back contact PSCs to act as semi-transparent devices when thin layers of perovskite absorber are employed. The average visible transmittance (AVT) is calculated between 400 and 800 nm for comparison to previously reported work. For the thinnest perovskite layer needed for the PSC to be operational, *viz.* 250 nm, which is the thickness of the back-contact electrode, a potential AVT of 32% was calculated. Corresponding PCE values were predicted as 5.9 and 7.5% for the devices irradiated from the front and rear, respectively (Table S6). These values are comparable to previous reports for tandem organic photovoltaics. At the maximum efficiencies, AVTs of 9.1% (front illumination, PCE = 12%) and 11% (rear illumination, PCE = 13%) were calculated, demonstrating potentially superior performance. The back-contact architecture also permits the application of an antireflective coating, light trapping, surface passivation, and photoluminescence out-coupling enhancements, which are expected to improve both the PCE and AVT of an optimized device.

To identify the contribution to charge collection efficiency across the spectrum, the external quantum efficiency (EQE) of the BC-PSC at the optimal conditions for front- and rearillumination was simulated (Figure 5b). In the short wavelength range (up to 430 nm), front-illumination is more efficient due to the absence of any parasitic absorption layer (ITO) in the first optical path of the incoming photons. In contrast, with rear illumination, the collection efficiency is higher within the higher wavelength range (430–780 nm), resulting in an increased accumulated J_{sc} . This is partly due to better index-matching between the glass|ITO|perovskite interfaces than the air|perovskite interface, effectively creating an anti-reflective coating that minimizes total reflectance. This leads to increased absorption in the perovskite, and a higher charge photogeneration rate near the back-contact electrode (Figure 5c). An order of magnitude

difference for the rear and front illumination conditions explains the experimentally observed difference in J_{sc} (Figure 4a and Table S5).

Simulations undertaken herein suggest that further optimization of devices with t-QIDEs should be possible by minimizing parasitic losses. For example, this can be achieved by increasing the pitch size, if possible with the given quality of perovskite material (*e.g.* with minority–carrier diffusion length $L_{\rm D} > 10~\mu{\rm m}$) (Figure S10a). Alternatively, increasing a filling fraction of the back-contact electrode is seen as a promising strategy for a realistic quality of perovskite ($L_{\rm D} \approx 0.5~\mu{\rm m}$). Unlike devices incorporating metal electrodes, the PCE is less sensitive to the width of the ITO back-contact finger (Figure S10b).¹⁶

In summary, the fabrication of a transparent back-contact electrode was achieved by replacing the opaque components of conventional QIDEs with ITO. These electrodes were used as substrates for the first semi-transparent back-contact perovskite solar cells with a modest PCE of 1.2%. Importantly, this new class of devices offers straightforward strategies for optimization that could significantly increase the efficiency. Simulations showed that if these improvements can be achieved, BC-PSCs incorporating t-QIDEs will offer a pathway to semitransparent photovoltaic devices.

Acknowledgements

We gratefully acknowledge the financial support from the National Science Foundation, NSF EAGER 1665279. G. D. is grateful for support from the NSF EAPSI program, OISE 1713327; E. R. thanks the Georgia Institute of Technology for support. E. R. additionally appreciates support from the Brook Byers Institute for Sustainable Systems at Georgia Tech.

This work was performed in part at the Melbourne Centre for Nanofabrication (MCN) in the Victorian Node of the Australian National Fabrication Facility (ANFF). A. N. J. acknowledges an Office of the Chief Executive Postdoctoral Fellowship (CSIRO Manufacturing). Y. H. acknowledges funding from the DFG Excellence Cluster "Nanosystems Initiative Munich" (NIM), the Center for NanoScience (CeNS) and the Bavarian Collaborative Research Program "Solar Technologies Go Hybrid" (SolTech). The authors thank Mr. Mark Greaves and Dr Aaron Seeber from CSIRO Manufacturing for their help with SEM imaging and x-ray analysis, respectively. E.C.G and G.W.P.A. acknowledge financial support from the European Research Council under the European Union's Seventh Framework Programme (FP/2007-2013)/ERC Grant Agreement 337328, "NanoEnabledPV".

References

- 1. Yoshikawa, Kunta, et al. "Silicon heterojunction solar cell with interdigitated back contacts for a photoconversion efficiency over 26%." Nature Energy 2 (2017): 17032.
- 2. Ma, Teng, et al. "Unveil the Full Potential of Integrated-Back-Contact Perovskite Solar Cells Using Numerical Simulation." ACS Applied Energy Materials (2018).
- 3. Jumabekov, A. N., et al. "Back-contacted hybrid organic-inorganic perovskite solar cells." Journal of Materials Chemistry C 4.15 (2016): 3125-3130.
- 4. Lu, Guilin, et al. "Development of back- junction back- contact silicon solar cells based on industrial processes." Progress in Photovoltaics: Research and Applications 25.6 (2017): 441-451.
- 5. H.L. Hartnagel, A.L. Dawar, A.K. Jain, C. Jagadish, Semiconducting Transparent Thin Films (Institute of Physics, Philadelphia, 1995)
- 6. Adhyaksa, Gede WP, Eric Johlin, and Erik C. Garnett. "Nanoscale back contact perovskite solar cell design for improved tandem efficiency." Nano letters 17.9 (2017): 5206-5212.
- 7. Helander, M. G., et al. "Chlorinated indium tin oxide electrodes with high work function for organic device compatibility." Science 332.6032 (2011): 944-947.
- 8. Yan, L. T., and R. E. I. Schropp. "Changes in the structural and electrical properties of vacuum post-annealed tungsten-and titanium-doped indium oxide films deposited by radio frequency magnetron sputtering." *Thin Solid Films* 520.6 (2012): 2096-2101.

- 9. Gupta, R. K., et al. "High mobility W-doped In 2 O 3 thin films: Effect of growth temperature and oxygen pressure on structural, electrical and optical properties." *Applied Surface Science* 254.6 (2008): 1661-1665.
- 10. Saliba, Michael, et al. "Cesium-containing triple cation perovskite solar cells: improved stability, reproducibility and high efficiency." Energy & Environmental Science 9.6 (2016): 1989-1997.
- 11. Calado, Philip, et al. "Evidence for ion migration in hybrid perovskite solar cells with minimal hysteresis." Nature communications 7 (2016): 13831.
- 12. Brongersma, Mark L., Yi Cui, and Shanhui Fan. "Light management for photovoltaics using high-index nanostructures." Nature materials 13.5 (2014): 451.
- 13. Roldán-Carmona, Cristina, et al. "High efficiency single-junction semitransparent perovskite solar cells." Energy & Environmental Science 7.9 (2014): 2968-2973.
- 14. Della Gaspera, Enrico, et al. "Ultra-thin high efficiency semitransparent perovskite solar cells." Nano Energy 13 (2015): 249-257.
- 15. Chen, Chun-Chao, et al. "High-performance semi-transparent polymer solar cells possessing tandem structures." Energy & Environmental Science 6.9 (2013): 2714-2720.
- 16. Knight, Mark W., et al. "Soft imprinted Ag nanowire hybrid electrodes on silicon heterojunction solar cells." Nano Energy 30 (2016): 398-406.